Holocene relative sea level changes and their consequences for the development of the palaeoshoreline in central Svalbard

Martin Lulák[1,2*], Daniel Nývlt[1,3], Milan Novák[4], Jan Kavan[1,2]

[1]*Polar-Geo Lab, Faculty of Science, Masaryk University, Kotlářská 267/2, 611 37 Brno, Czech Republic*
[2]*Centre for Polar Ecology, Faculty of Science, University of South Bohemia, Na Zlaté stoce 690/3, 370 05 České Budějovice, Czech Republic*
[3]*Czech Geological Survey, Brno Branch, Leitnerova 22, 658 69 Brno, Czech Republic*
[4]*Department of Computer Science, Faculty of Science, University of South Bohemia, Branišovská 1645/31a, 370 05 České Budějovice, Czech Republic*

Abstract
The Arctic, particularly the Barents Sea region including Svalbard, has undergone exceptional warming and environmental change throughout the Holocene. This study investigates Holocene relative sea level (RSL) changes in Petuniabukta, northern Billefjorden (Svalbard), using radiocarbon dated whale bones found on uplifted marine terraces as indicators of past shoreline positions. Five new samples from the western side of the bay were integrated with previously published data from the eastern side to reconstruct palaeoshorelines and quantify land emergence driven by glacioisostatic rebound. The two oldest samples, located at 58.1 m a.s.l. and 34.7 m a.s.l., date at 10.3 and 9.1 cal. ka BP respectively, indicate rapid Early Holocene uplift averaging 3 cm/year. Spatial analysis based on ArcticDEM and high-resolution UAV-derived models reveals a 33% reduction in the marine area since the Early Holocene, with significant changes occurring in broad glaciated valley regions. Discrepancies in RSL trends may be attributed to local tectonic activity along the Billefjorden Fault Zone. While Early Holocene changes are well constrained, Late Holocene and Neoglacial sea-level dynamics remain ambiguous due to a lack of preserved indicators and minimal RSL variation. These findings highlight the potential of stranded whale bones as precise RSL markers and contribute to understanding the long-term cryospheric and geomorphic evolution of coastal areas in a rapidly warming Arctic.

Key words: coastline, Early Holocene, whale bones, glacioisostatic rebound, marine terraces

DOI: 10.5817/CPR2025-S-7

Received January 15, 2025, *accepted* August 28, 2025.
*Corresponding author: M. Lulák <lulakm00@prf.jcu.cz>
Acknowledgements:
This work was supported by the project 'ARCTOS MU' (MUNI/G/1540/2019), funded by the Grant Agency of Masaryk University (GAMU), and the project MUNI/A/1469/2023. Fieldwork and radiocarbon dating were provided by the project 'Polar Ecology Course – Geosciences' (NF-CZ07-ICP-1-032-2014), funded by EEA grants and CzechPolar2 (LM2015078).
We would like to acknowledge the help of Zdeněk Stachoň and Zbyněk Engel for post-processing the dGPS data. We also thank to the editors and anonymous reviewers for the insightful comments that improved the manuscript.

***Abbreviations**:* BP – before present, DEM – digital elevation model, GCP – ground control points, GPS – global position system, LIA – little ice age, m a.s.l. – metres above sea level, RSL – relative sea level, UAV – unmanned aerial vehicle

Introduction

In last few decades, the Arctic is one of the most dynamic geosystems on Earth in its response to global climate change. It has been warming four times faster than the global average in recent decades. This rapid warming is driven by a set of positive feedbacks, often referred to as Arctic amplification (Rantanen et al. 2022). Moreover, the Barents Sea region, including Svalbard, has been warming twice as fast as the Arctic average (Isaksen et al. 2022, Nordli et al. 2020). However, present-day dynamics are comparable to abrupt environmental changes observed throughout the Holocene (van der Bilt et al. 2019). The landscape visible today is therefore the result of complex geosystem development over the past 10–12 thousand years.

Environmental reconstructions suggest exceptional regional warmth in Svalbard during the Pleistocene–Holocene transition (12.0–10.5 ka BP), which led to rapid fjord system deglaciation (Mangerud and Svendsen 2018, Farnsworth et al. 2020). The actual sea level at the beginning of the Holocene may have been up to 70 m higher than today's in some areas around Svalbard (*e.g.* Nordaustlandet; Salvigsen 1977). However, relative sea level (RSL) change is highly spatially variable around Svalbard due to uneven glacioisostatic uplift following deglaciation. As a result, reported RSL changes since 10.5 ka BP range from 50 m in NE Svalbard (Schomacker et al. 2019) to 70 m in N Svalbard (Farnsworth et al. 2024), 20 m in W Svalbard (Farnsworth et al. 2017) and less than 10 m in the south (Stachowska et al. 2024). Forman et al. (2004) reported 27 RSL change records from sites around Svalbard corresponding to c. 9.0 ka BP, with an average of 27.9 ± 21.1 metres above sea level (m a.s.l.).

The Holocene glacial minimum in Svalbard culminated in the Mid-Holocene (~8.0–6.0 ka BP), and no glacial landforms corresponding to glacier readvances or still-stands have been identified between 9.0 and 4.5 ka BP (Farnsworth et al. 2020). Late Holocene glacier readvances, linked to episodic Neoglacial cooling terminating in the Little Ice Age (LIA), have been dated to 4.0–0.5 ka BP, with the greatest advances occurring between 1.0 and 0.5 ka BP (Farnsworth et al. 2020). Since the end of the LIA (~1900 CE; Szczuciński et al. 2009), Svalbard glaciers have experienced widespread negative mass balance and retreat with up to 19.1% reduction in their extent since LIA in western and central Spitsbergen (Martín-Moreno et al. 2017). Small valley-type glaciers adjacent to our study site have lost more than 90% of their volume since 1930s (Kavan 2020a; McCerery et al., *in review*). Such rapid ice mass loss may lead to further acceleration of glacioisostatic uplift in the near future.

Climate dynamics, consequent glacier ice mass loss and resulting glacioisostatic uplift have created a unique setting for the preservation of various accumulation coastal landforms. Typical sentinels of past climate and geosystem dynamics include marine terraces (*e.g.* Sessford et al. 2015) and deltas (Yoshikawa and Nakamura 1996). Uplifted marine terraces are widespread along Arctic coastlines, including central Canadian Arctic (*e.g.* Dyke et al. 1991), Russian Arctic coast and archipelagos (*e.g.* Baranskaya et al. 2018), as well as all around the coast of Greenland (*e.g.* Weidick 1972) and their sediments serve as key sources of information on glacioisostatic rebound, RSL changes, and past ice volume estimates in Svalbard (*e.g.* Boulton 1979, Mangerud and Salvigsen 1984, Mangerud and Svendsen 1992, Long et al. 2012, Sessford et al. 2015). Marine shells, driftwood and whale bones are commonly used to date these terraces. Driftwood and whale bones are often preferred, as marine shells may be reworked if not found in living position (Dyke et al. 1991, Bondevik et al. 1995, Forman et al. 2004).

Most marine mammals, including whales, die at sea, and their bones typically sink to the sea floor. However, some species such as the Greenland whale (*Balaena mysticetus*) are extremely fat (Dyke et al. 1991, 1996), and their carcasses can float for weeks or even months before washing ashore (Bennike and Wagner 2021), where they may be stranded on beaches and then uplifted by glacioisostatic rebound. Alternatively, beaching of live whales may occur due to illness, injury, bad weather, old age or navigation errors (Barr 1971). In both cases, the carcass becomes lodged in the coastal zone, which essentially has a null height relative to mean sea level. This makes whale bones, especially if large parts of the skeleton are preserved, excellent indicators of former sea level position.

Such phenomena have also been observed at the present study site. In 2012, an individual of the sperm whale (*Physeter macrocephalus*) stranded in the littoral zone of the eastern part of Petuniabukta (Figs. 1C and 2F). Between summer 2012 and summer 2015, the carcass disintegrated, and its bones became buried in sediment close to the shore.

The well-preserved sequence of marine terraces on the western side of Petuniabukta, including its uppermost part, creates a favourable setting for whale bone deposition and the study of RSL changes. The main questions addressed in this study are as follows:

1) How did glacioisostatic rebound operate in Petuniabukta during the Early Holocene?;

2) How did the shoreline evolve from the Holocene to the present day?;

3) How much of Petuniabukta's current land area was below sea level during the Holocene?;

4) How did glacier advances during the Neoglacial and, in particular, the LIA transform previously submerged zones in northern Billefjorden?

The aim of this paper is to contribute to reconstructing Holocene changes in relative sea level. We hypothesised that it would be possible to answer the above-specified questions by whale bone dating.

Material and Methods

Study site

Petuniabukta (Fig. 1) and its marine terraces were previously studied by Long et al. (2012) and Sessford et al. (2015). However, their findings are limited to the Ebba Valley on the eastern side of Petuniabukta. Their RSL data indicate the highest terrace at 28 m a.s.l., with an age of 9.7 ± 0.2 cal. ka BP, and the lowest terrace at approximately 1 m a.s.l., with an age of 3.1 ± 0.2 cal. ka BP (Long et al. 2012; both ^{14}C ages calibrated by the authors). The RSL during the Holocene therefore reached a level within a metre of the present sea level by c. 3.1 cal. ka BP, which suggests that the late Holocene RSL fell below the present level and rose again in the last millennium (Long et al. 2012). These findings were used to supplement data from the western side of Petuniabukta, particularly from 20 m a.s.l. (~8.3 cal. ka BP) to the present level.

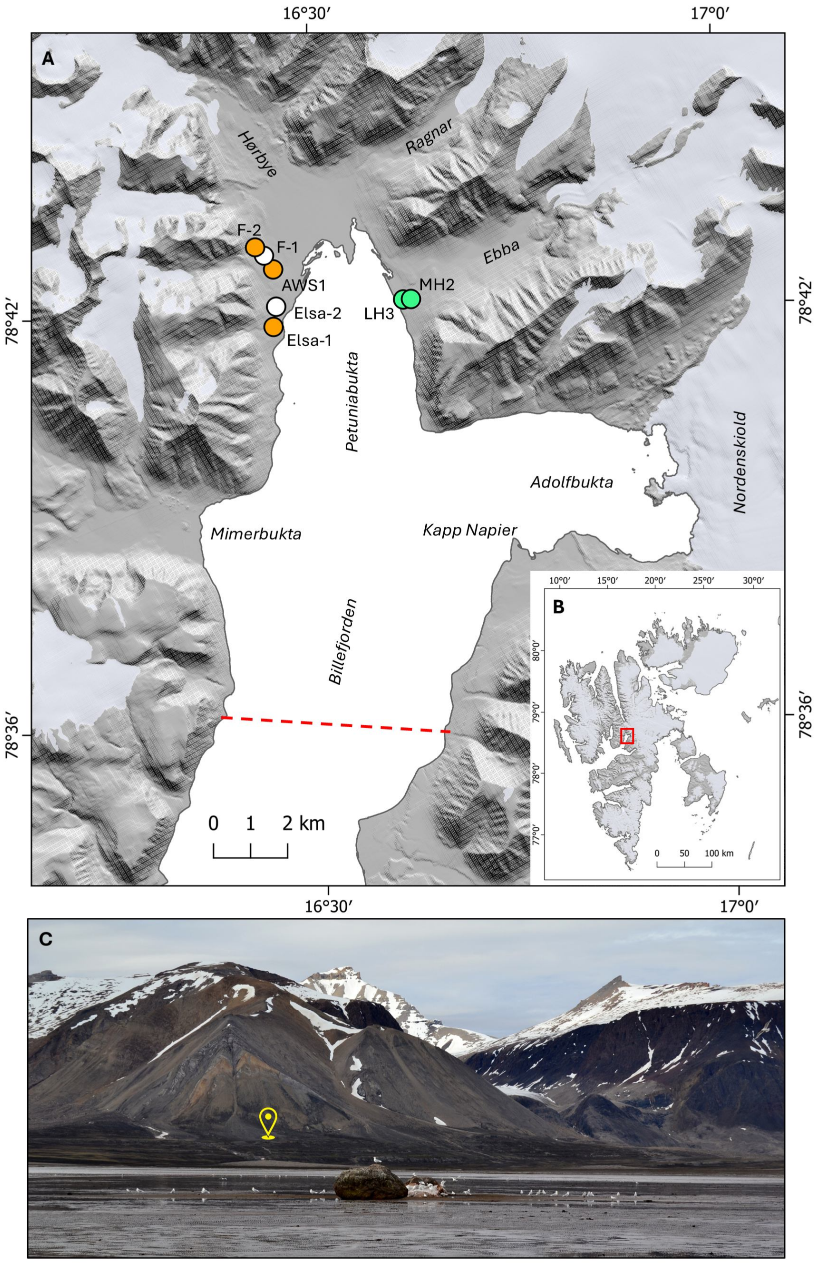

Fig. 1. (**A**) Billefjorden area with locations of samples used for the analyses of RSL change and sea extent; whale bone samples on the western side of Petuniabukta with orange highlighted samples used in sea extent analyses; green shell samples from Long et al. (2012), red dashed line indicates southern limit of studied coastal zone; (**B**) Svalbard with highlighted terrain configuration and glacier coverage (in light blue tones), red rectangle limits the extent of panel A; (**C**) boulder with carcass of the sperm whale stranded in Petuniabukta (on the shore of Ebba valley) in 2012 in the foreground, sequence of beach terraces with location of the highest positioned whale bone sample highlighted with a yellow tag; photo taken during low tide.

Sampling and radiocarbon dating

Five whale bone samples were collected from five different localities on the western side of Petuniabukta (Figs. 1 and 2). The altitudes and locations of all whale bones were measured using a standard GPS calibrated to the present mean sea level altitude on the day of sampling. All altitudes were also cross-checked with ArcticDEM (Porter et al. 2023) and adjusted to fit the digital elevation model (DEM) if necessary. The altitudes of the samples from Long et al. (2012) were determined by them via onsite optical levelling. The largest discrepancy between the handheld GPS and DEM values was observed for the Elsa-2 sample (2.35 m), while the three samples used for palaeoshoreline reconstruction showed negligible differences (0.95 m, 0.1 m and 0.2 m for Elsa-1, AWS1 and F-2, respectively).

The ages of all five whale bones from western Petuniabukta were determined via the Accelerator Mass Spectrometry ^{14}C method at the Poznań Radiocarbon Laboratory, Poland. For the eastern part of Petuniabukta (Ebba Valley), two previously published ages (samples LH3 and MH2; Long et al. 2012) were used. All radiocarbon ages were calibrated using the Marine20 dataset (Heaton et al. 2020) and expressed relative to the year 1950 CE, that is, as cal. BP (Stuiver and Polach 1977), applying a local marine radiocarbon reservoir correction ΔR of –56 ± 33 a BP. This value is based on six points located around Svalbard (Mangerud 1972, Mangerud and Gulliksen 1975, Olsson 1980) from the Marine20 Database. All ^{14}C results with their corresponding altitudes are listed in Table 1.

locality		GPS	m asl (GPS)	m asl (DEM)	lab no.	^{14}C age	cal. age (2 σ)	cal. min. age (2 σ)	cal. max. age (2 σ)
Elsa-1	this study	N78°41'50.3"; E016°27'00.1"	19	19.95	Poz-128830	7980 ± 50 BP	8337 ± 179 cal. BP	8158	8516
Elsa-2	this study	N78°42'07.8"; E016°27'13.9"	14	11.65	Poz-128831	8180 ± 50 BP	8570 ± 211 cal. BP	8359	8780
AWS1	this study	N78°42'40.3"; E016°27'04.7"	22	21.9	Poz-128832	8570 ± 50 BP	9086 ± 219 cal. BP	8867	9305
F-1	this study	N78°42'52.6"; E016°26'25.5"	35	34.7	Poz-128833	8770 ± 50 BP	9308 ± 188 cal. BP	9120	9496
F-2	this study	N78°43'00.1"; E016°25'46.8"	58	58.1	Poz-129051	9510 ± 50 BP	10294 ± 206 cal. BP	10088	10500
LH3	Long et al. 2012	*n/a*	*n/a*	5.01	SUERC-35209	4545 ± 37 BP	4622 ± 190 cal. BP	4432	4812
MH2	Long et al. 2012	*n/a*	*n/a*	16.26	SUERC-35212	7298 ± 39 BP	7637 ± 161 cal. BP	7476	7797

Table 1. Overview of the samples used in the study. Orange highlighted samples used in sea extent analyses; green shell samples from Long et al. (2012). The altitudes of the LH3 and MH2 samples were determined via onsite optical levelling.

Spatial analysis

A 2 m resolution ArcticDEM mosaic (tile ID: 35_51_2_1) was used to derive actual contour lines for the samples included in the analysis: LH3, MH2 (from Long et al. 2012), and Elsa-1, AWS1, and F-2 (from the present study) at 0, 5, 16, 20, 22 and 58 m a.s.l. This was complemented by two subglacial bedrock topography models to assess whether areas currently occupied by glaciers may have been submerged in the past. The datasets used were from Fürst et al. (2018) and van Pelt and Frank (2025). The ArcticDEM was corrected with a single offset value to account for the difference between ellipsoid and geoid data, aligning with the actual zero seawater level. The procedure is described in detail by Kavan et al. (2022). Marine terrace cross-sections were obtained using the terrain "profile tool" plugin applied to the unmanned aerial vehicle (UAV)-based DEM (*see* below). All spatial analyses were performed in QGIS 3.34.

High-resolution DEM and orthophoto construction

A UAV, DJI Mavic 3 Pro, was used to map the marine terraces in front of the Ferdinand (N 78°42'30'', E 16°20') and Elsa glaciers (N 78°41', E 16°22'). The survey was conducted on 22 July 2024 around noon to minimise shadowing. A total of 3,283 photographs were taken from a fixed altitude of 120 m above the starting point, with frontal and side image overlaps set to 80% and 70%, respectively. The flight mission was planned directly within the DJI application using available satellite imagery and prior field reconnaissance.

The photographs were processed in Pix4Dmapper (Pro version 3.0.18) to produce the final orthophoto and DEM, with a spatial resolution of 5 cm per pixel. A network of six ground control points (GCPs) was used for georeferencing. Large standalone rocks or other distinctive objects (*e.g.* driftwood, stranded litter) identifiable in the images were selected as GCPs. GCPs were evenly distributed across the study area to ensure accurate positioning of the orthophoto and DEM. The position of each GCP was recorded using a Trimble Geo7x differential GPS for at least 90 seconds to ensure high precision. The measured dGPS data were corrected using Trimble Pathfinder Office software (ver. 5.81; Release Notes for TRIMBLE, 2015).

Results and Discussion

The most complete whale remains, including a series of vertebrae and ribs, were localised at Petuniabukta locations F-2 (58 m a.s.l.; Fig. 2E) and AWS1 (22 m a.s.l.; Fig. 2C). In other localities, only a few bones were found (partially buried in the sediment), and their altitude was considered less relevant or precise. All samples were collected from bones located on the surface of marine terraces. The calibrated ages and altitudes (in m a.s.l.) are listed in Table 1.

Samples Elsa-1 and Elsa-2 were statistically the same age (8.3 ± 0.2 cal. ka BP and 8.6 ± 0.2 cal. ka BP, respectively), even though their altitudes above sea level differ. It is assumed that the lower bone (Elsa-2) was resedimented over time to its current altitude. A similar situation applies to samples F-1 and AWS1 (9.3 ± 0.2 cal. ka BP and 9.1 ± 0.2 cal. ka BP, respectively). Considering the difference in condition between these two samples (AWS1 features a much more complete skeleton), it is suspected that the single bone was transported higher, for example, by scavengers. In both cases, it cannot be ruled out that the paired samples belong to the same individuals.

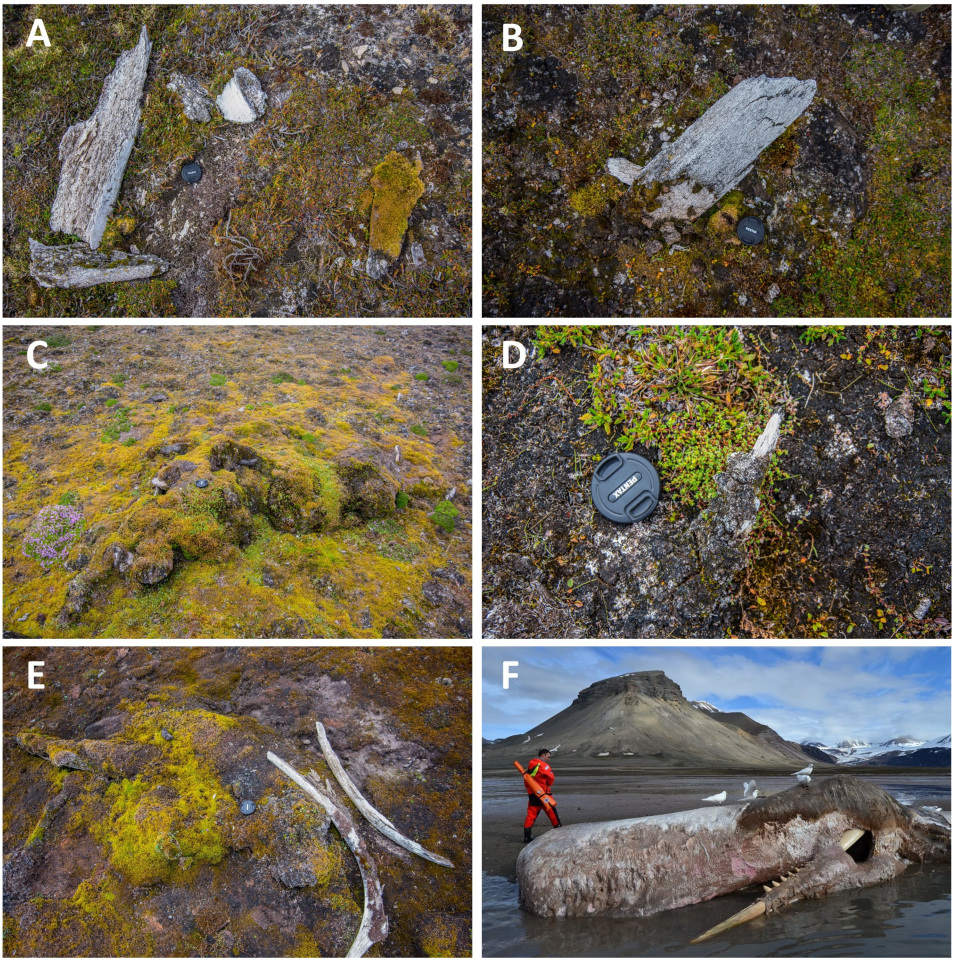

Fig. 2. Sampled whale bones from the western shoreline in Petuniabukta. **A** – Elsa-1; **B** – Elsa-2; **C** – AWS1; **D** – F-1; **E** – F-2; **F** – Example of a beached carcass of a sperm whale (*Physeter macrocephalus*) on the eastern shore of the same area (shoreline of Ebba valley, Petuniabukta) in 2012.

Palaeoshorelines

The positions of potential palaeoshorelines are illustrated in Fig. 3. The potential shoreline at 58 m a.s.l., representing the 10.3 cal. ka BP shoreline, delimits a significantly larger areal extent of the sea. The sea occupied 130 km², whereas it currently occupies only 87.5 km², which represents an almost 33% decrease in the marine environment in northern Billefjorden during the Holocene (Fig. 4). The most notable differences from the present-day shoreline are found in the flat areas of large glacial valleys – namely, the Hørbye, Ragnar, Ebba and Mimer valleys. Significant differences also appear in the locality of Kapp Napier, where a sequence of Holocene raised beach ridges is located.

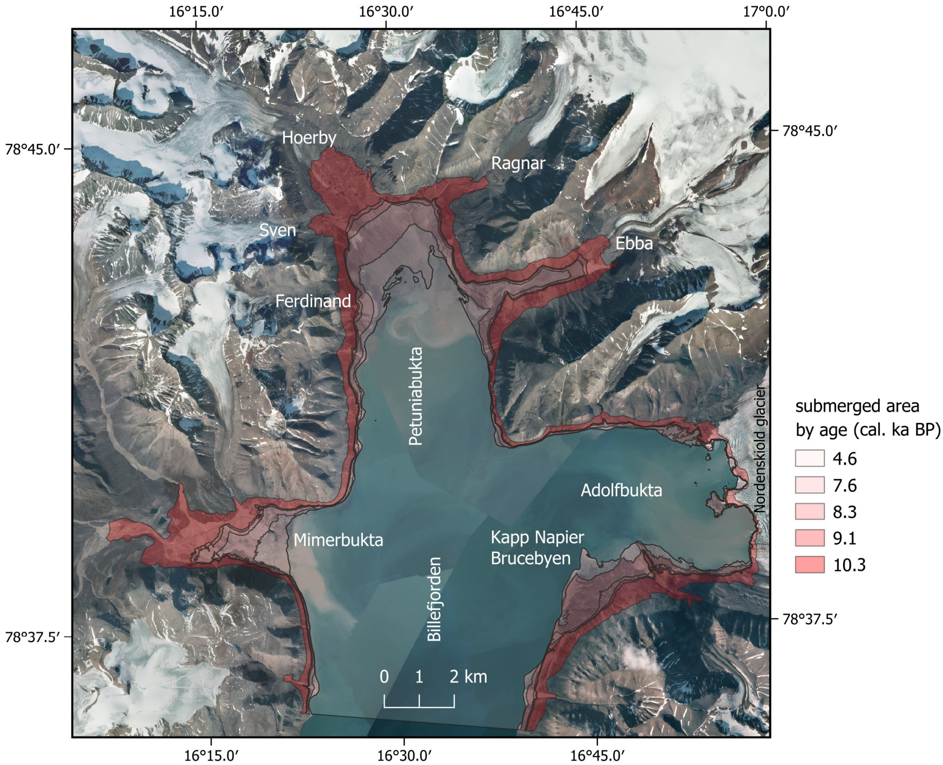

Fig. 3. Submerged area in Petuniabukta, Adolfbukta and Mimerbukta by age.

The submerged area declined rapidly during the Early Holocene, specifically between 10.3 and 9.1 cal. ka BP. This corresponds to the highest reported RSL change, resulting from massive ice cap decay and land unloading. Average RSL change between our two samples (AWS1, 9.1 cal. ka BP and F-2, 10.3 cal. ka BP) is ca 3 cm/year. This is in good correspondence with other studies from the Svalbard region – 1 to 3.1 cm/year in Early Holocene according to *e.g.* Salvigsen (1981), Salvigsen and Österholm (1982), Forman et al. (2004) or Möller (2024). The 9.1 cal. ka BP sample appears slightly outside the smoothed curve. This may be due to the local topographic configuration of marine terraces predisposed by bedrock outcrops, which results in an irregular relationship between sea level fall and corresponding areal extent. The response of glaciers to Holocene warming has also been nonlinear (Jang et al. 2023). Another possible explanation for this deviation may lie in the position of Billefjorden within the major tectonic fault zone – the Billefjorden Fault Zone (Koehl and Allaart 2021). Vertical movements along the fault may have been discontinuous, causing discrepancies in the RSL changes. The Early Holocene land emergence and rapid glacier ice mass loss may have triggered local earthquakes (Auer et al. 2025), significantly affecting uplift rate dynamics. A major earthquake dated to c. 9.5 cal. ka BP was identified in the lake sediment record north of the Billefjorden area (Auer et al. 2025). A similar event in the fault zone was also recorded as recently as 2008 (Ottemöller et al. 2021).

In contrast, the development of coastal zones during the Neoglacial remains unclear, as no preserved physical samples are available. This may be due to a short-lived transgression since c. 3 ka BP as a result of regional cooling (Farnsworth et al. 2020). Similar findings have been reported from NW Svalbard (Forman 1990, Fjeldskaar et al. 2018). Subsequent loading of ice in ice caps and glaciers may have reversed the direction of glacioisostatic movement (Long et al. 2012, Farnsworth et al. 2020), which had been the major driver of RSL change for most of the Holocene. This interpretation is supported by the dating of shells in the Ebba Valley, where samples dated to c. 3 ka BP have altitudes very similar to modern samples dated to the end of the LIA (Long et al. 2012). Signs of seawater intrusion were also identified in shallow sediment cores from ponds in the coastal zone of Kapp Napier (unpublished data of the authors). Temporary seawater intrusion into the flat coastal zone may have serious consequences for the physicochemical properties of initial soils exposed after glaciers retreat from their maximum LIA extent. The characteristics of the initial substrate were found to be crucial for the further development of soils in front of the Nordenskiöld Glacier (Luláková et al. 2023, Tejnecký et al. 2025).

The potentially submerged area at the beginning of the Holocene (corresponding to the F-2 sample at 58 m a.s.l.) was likely larger than the area derived from a simple DEM analysis, as shown in Fig. 4. The freshly exposed landscape, following the rapid retreat of ice streams and glaciers, was eroded and lacked the accumulative landforms left by the glacier advance during the LIA (*e.g.* push moraines and till plains). Slope deformation leading to the formation of large talus cones and alluvial fans limited the areal extent of valley bottoms during the Holocene and particularly during the Neoglacial and LIA (Tomczyk 2021). As a result, the freshly deglaciated valleys at the beginning of the Holocene were probably wider, and the submerged area correspondingly larger.

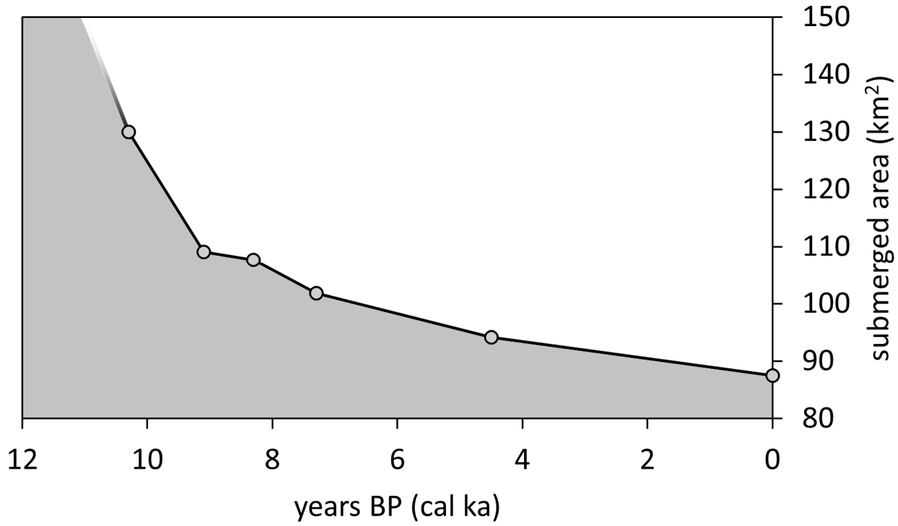

Fig. 4. Submerged area by age.

A similar effect was likely produced by the Neoglacial and LIA advance of individual glaciers, which led to the formation of massive frontal moraines that restricted the valleys transversely (Rachlewicz et al. 2007, Martín-Moreno et al. 2017). This situation is clearly demonstrated in the case of the Ebba glacier, where at 10.3 cal. ka BP, the extent of the submerged area is limited precisely to the foot of the LIA frontal moraine. The sea likely expanded well beyond the present moraine. The same applies to the Ragnar glacier, which currently hosts a vast proglacial lake dammed by a frontal moraine (*see*, e.g. Ewertowski and Tomczyk 2020). The SVIFT subglacial topography model indicates bedrock below the 58 m a.s.l. threshold at the glacier terminus. This is supported by lake bathymetry data, which also indicate that the lake bottom at maximum depth corresponds to approximately 55–60 m a.s.l. (unpublished data of the authors). Thus, it can be assumed that the submerged area extended towards the present glacier terminus, as illustrated in Fig. 5.

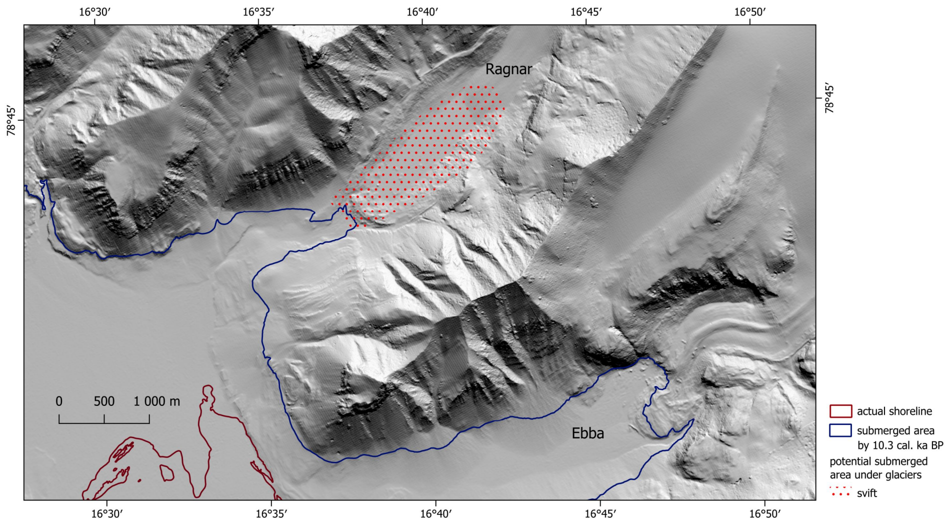

Fig. 5. Potentially submerged area under Ragnar glacier; ArcticDEM shaded relief as a background to highlight the terrain features (DEM data from Porter et al. 2023); SVIFT subglacial topography model (Fürst et al. 2018).

A similar effect can be observed in the case of the Hørbye glacier (Fig. 6), which has deposited large amounts of (sub)glacial till along with lateral and frontal moraines (Evans et al. 2012). The present-day landscape probably originated from a surge-type behaviour of the glacier (Małecki et al. 2013). As indicated by both the SVIFT and van Pelt and Frank subglacial topography models, the submerged area extended further into the valley, most likely limiting the sea extent at the foot of the present-day roche moutonée. In reality, the submerged area was therefore significantly larger than the DEM analysis revealed.

The submerged area in front of the Sven glacier has extended towards the roche moutonée, with the present-day basal moraine area submerged. The Ferdinand glacier probably also extended close to the shoreline at the beginning of the Holocene. This is supported by the formation of alluvial fans or deltas directly at the foot of the current LIA frontal moraine

(Strzelecki et al. 2018), which corresponds to the potential sea level at the 10.3 cal. ka BP sample (58 m a.s.l.).

Similarly, one would expect a large submerged area beneath the Nordenskiöld glacier, which is presently terminating directly into Adolfbukta. However, the glacier is currently undergoing a transition from marine- to land-terminating, that is, losing its ice calving front. Recently, only the southern basin shows signs of calving (summer 2025 observation by authors), whereas the northern basin is completely land-terminating since 2017 (Kavan et al. 2024). The bedrock topography is also not favourable for extensive submersion due to large and relatively high bedrock outcrops near the present-day terminus. Some of these outcrops have already been exposed, supporting the validity of the SVIFT model outcomes. The bedrock topography model by van Pelt and Frank (2025) indicates a potentially large area available for submersion in the southern margin region (Fig. 7).

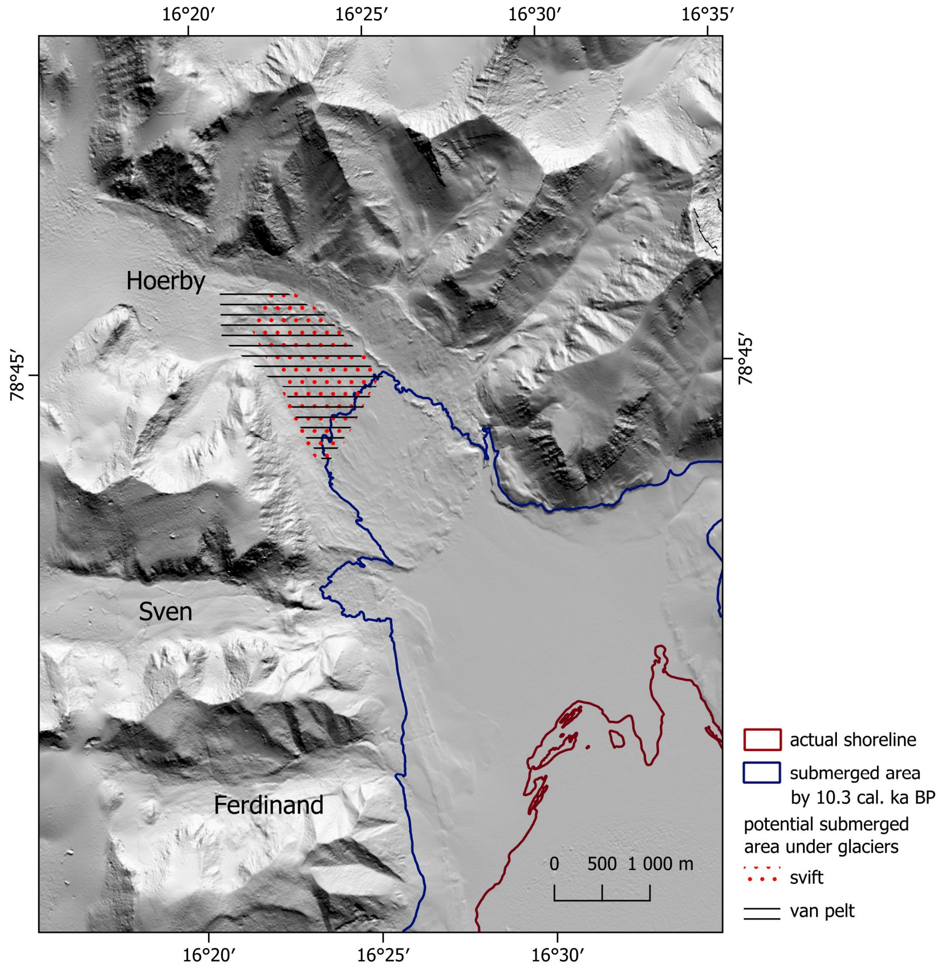

Fig. 6. Potentially submerged area under Hørbye glacier; ArcticDEM shaded relief as a background to highlight the terrain features (DEM data from Porter et al. 2023); SVIFT subglacial topography model (Fürst et al. 2018) and "van pelt" subglacial topography model (van Pelt and Frank 2025).

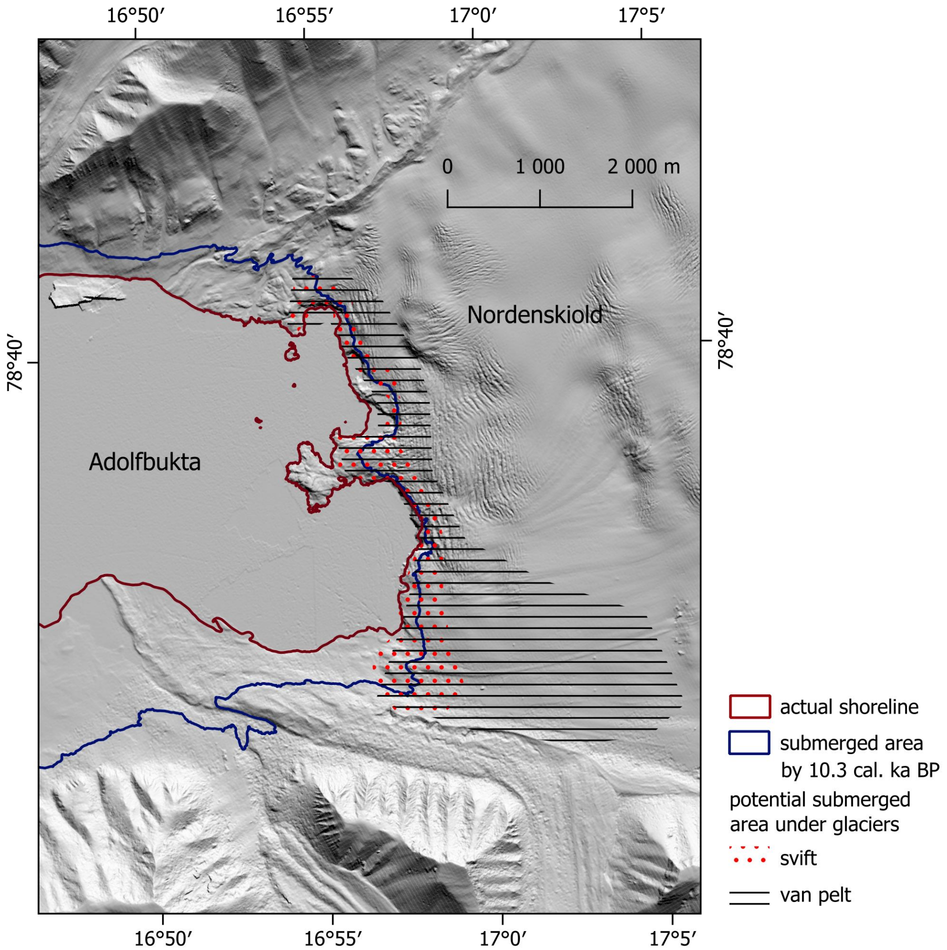

Fig. 7. Potentially submerged area under the Nordenskiold glacier; ArcticDEM shaded relief as a background to highlight the terrain features (DEM data from Porter et al. 2023); SVIFT subglacial topography model (Fürst et al. 2018) and "van pelt" subglacial topography model (van Pelt and Frank 2025).

However, this does not match the physical evidence from the site. The model's reported uncertainties are highest near the calving fronts, which further supports the field observations. In this case, the SVIFT model seems to represent reality more accurately.

Although the Nordenskiöld glacier is unlikely to expose large new coastal areas, significant fluctuations were reported during the Holocene across Svalbard (Forman et al. 2004), and more specifically in certain locations (Osika et al. 2022). Fluctuations, mainly retreats, have occurred around Svalbard since the LIA (Kavan and Strzelecki 2023), resulting in the exposure of fresh coastlines (*e.g.* Strzelecki et al. 2020). The advance and retreat of tidewater glaciers continue to influence the extent of exposed coastal zones across the Arctic in recent decades as well (Kavan et al. 2025), likely reflecting conditions similar to abrupt Early Holocene warming.

For Svalbard, the best example of continuous coastal landscape transformation throughout the Holocene can be found at Kapp Napier. The raised beach ridges illustrate the development of a sediment-rich supply system and the reworking of older marine terraces in recent decades (Kavan 2020b). Rapid progradation of the beach ridges led to the formation of several cut-off lakes. The most recent process, which began around 2010–2020 (Kavan and Hanáček 2025; *this issue*), is a close analogue of the earlier processes responsible for the formation of the old, stabilised lakes at altitudes of 5–6 m a.s.l. (*i.e.* c. 5 cal. ka BP) in the present-day settlement of Brucebyen.

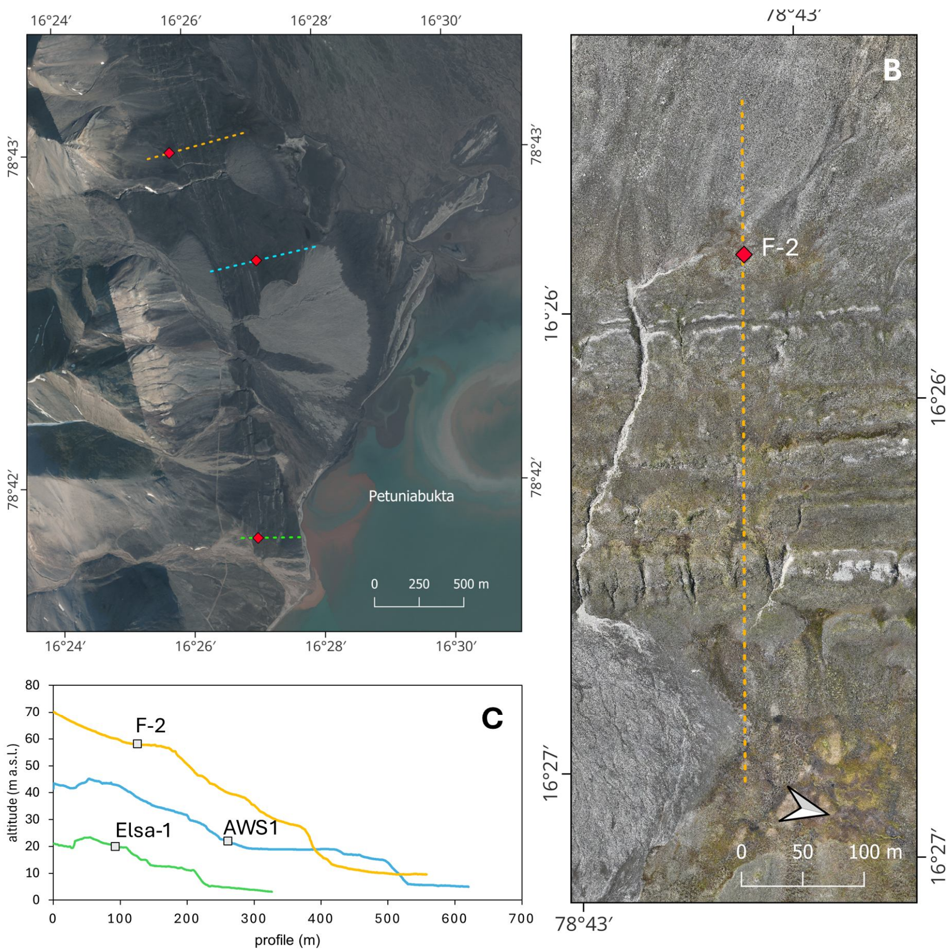

Fig. 8. Cross sections through the marine terraces at the three sites used for palaeoshoreline reconstruction; (**A**) western side of Petuniabukta with the locations of all three sites and cross sections (NPI aerial image as a background); (**B**) close-up view of the F-2 site with high-resolution UAV image as a background; (**C**) cross profiles overlaid in one scheme.

Marine terraces cross-sections

The three whale bone samples used for constructing the RSL curve (F-2, AWS1, Elsa-1) are positioned on a sequence of Holocene marine terraces. These areas are, however, influenced by bedrock outcrops and do not form a smooth sequence of raised marine beach ridges, as seen in the Ebba Valley (Long et al. 2012) or Kapp Napier (Kavan and Hanáček 2025; *this issue*), for example. The bedrock topography and resulting discontinuous formation of the terraces may be a controlling factor contributing to the rather sketchy RSL curve.

The whale bones are typically located at the foot of a major terrain feature (*i.e.* bedrock outcrop; Fig. 8), which likely stabilised their deposition at a specific spot. For the palaeoshoreline analyses, we used these three samples with due to this characteristic pattern of deposition. Moreover, there was usually more than one single bone present at the site, suggesting that the site was the original location where the whales had stranded.

Conclusions

This study demonstrates the value of whale bone dating in reconstructing Holocene RSL changes. Notably, the sample from an altitude of 58 m a.s.l. (dated to 10.3 cal. ka BP) adds to the existing sea level curve established by earlier research in northern Billefjorden. When combined with detailed spatial analysis of the current terrain, the curve illustrates the evolution of shoreline positions throughout much of the Holocene and highlights the substantial land gain resulting from glacioisostatic rebound following the Pleistocene/Holocene deglaciation.

Many of today's glacier valleys were once submerged, including areas now occupied by glaciers. Land gained through Holocene glacioisostatic rebound – previously beneath the sea – may retain marine imprints in the physicochemical composition of its mineral material. These characteristics may have significantly shaped the Holocene terrestrial succession and biodiversity of the newly exposed areas.

References

AUER, A. G., VAN DER BILT, W. G. M., SCHOMACKER, A., BAKKE, J., STØREN, E. W. N., BUCKBY, J. M., CEDESTRØM, J. M. and VAN DER PLAS, S. (2025): Hydroclimate intensification aided Early Holocene Arctic glacier survival. *Communications Earth & Environment*, 6: 100. doi: 10.1038/s43247-025-02064-z

BAAR, W. (1971): Postglacial isostatic movement in northeastern Devon Island: A reappraisal. *Arctic*, 24: 249-268.

BARANSKAYA, A. V., KHAN, N. S., ROMANENKO, F. A., ROY, K., PELTIER, W. R. and HORTON, B. P. (2018): A postglacial relative sea-level database for the Russian Arctic coast. *Quaternary Science Reviews*, 199: 188-205. doi: 10.1016/j.quascirev.2018.07.033

BENNIKE, O., WAGNER, B. (2021): Quaternary vertebrates from the North Atlantic Islands. *In*: E. Panagiotukopulu, J. P. Sadler (Eds.): *Biogeography in the Sub-Arctic: The Past and Future of North Atlantic Biota*. pp. 147–160. doi: 10.1002/9781118561461.ch7

BONDEVIK, S., MANGERUD, J., RONNERT, L. and SALVIGSEN, O. (1995): Postglacial sea-level history of Edgeøya and Barentsøya, eastern Svalbard. *Polar Research*, 14: 153-180. doi: 10.3402/polar.v14i2.6661

BOULTON, G. S. (1979): Glacial history of the Spitsbergen archipelago and the problem of a Barents Shelf ice sheet. *Boreas*, 8: 31-57. doi: 10.1111/j.1502-3885.1979.tb00429.x

DYKE, A. S., MORRIS, T. F. and GREEN, D. E. C. (1991): Postglacial tectonic and sea level history of the central Canadian Arctic. *Geological Survery of Canada Bulletin*, 397, 56 p. 10.4095/132168

DYKE, A. S., HOOPER, J. and SAVELLE, J. M. (1996): A history of sea ice in the Canadian Arctic archipelago based on the postglacial remains of the bowhead whale (*Balanea mysticetus*). *Arctic*, 46: 235-255. doi: 10.14430/ARCTIC1200

EVANS, D. J. A., STRZELECKI, M., MILLEDGE, D. G. and ORTON, C. (2012): Hørbyebreen polythermal glacial landsystem, Svalbard. *Journal of Maps*, 8: 1-11. doi: 10.1080/17445647.2012.680776

EWERTOWSKI, M. W., TOMCZYK, A. M. (2020): Reactivation of temporarily stabilized ice-cored moraines in front of polythermal glaciers: Gravitational mass movements as the most important geomorphological agents for the redistribution of sediments (A case study from Ebbabreen and Ragnarbreen, Svalbard). *Geomorphology*, 350: 106952. doi: 10.1016/j.geomorph.2019.106952

FARNSWORTH, W. R., INGÓLFSSON, Ó., NOORMETS, R., ALLART, L., ALEXANDERSON, H., HENRIKSEN, M. and SCHOMACKER, A. (2017): Dynamic Holocene glacial history of St. Jonsfjorden, Svalbard. *Boreas*, 46(3): 585-603. doi: 10.1111/bor.12269

FARNSWORTH, W. R., ALLAART, L., INGÓLFSSON, Ó., ALEXANDERSON, H., FORWICK, M., NOORMETS, R., RETELLE, M. and SCHOMACKER, A. (2020): Holocene glacial history of Svalbard: Status, perspectives and challenges. *Earth Science Reviews*, 208: 103249. doi: 10.1016/j.earscirev.2020.103249

FARNSWORTH, W. R., INGÓLFSSON, Ó., BRYNJÓLFSSON, S., ALLAART, L., KJELLMAN, S. E., KJÆR, K. H., LARSEN, N. K., MACIAS-FAURIA, M., SIGGAARD-ANDERSEN, M. and SCHOMACKER, A. (2024): Persistence of Holocene ice cap in northeast Svalbard aided by glacio-isostatic rebound. *Quaternary Science Reviews*, 331: 108625. doi: 10.1016/j.quascirev.2024.108625

FJELDSKAAR, W., BONDEVIK, S. and AMANTOV, A. (2018): Glaciers on Svalbard survived the Holocene thermal optimum. *Quaternary Science Reviews*, 199: 18-29. doi: 10.1016/j.quascirev.2018. 09.003

FORMAN, S. L. (1990): Post-glacial relative sea-level history of northwestern Spitsbergen, Svalbard. *GSA Bulletin*, 102(11): 1580-1590.

FORMAN, S., LUBINSKI, D.J., INGÓLFSSON, Ó., ZEEBERG, J. J., SNYDER, J. A., SIEGERT, M. J. and MATISHOV, G. G. (2004): A review of postglacial emergence on Svalbard, Franz Josef Land and Novaya Zemlya, northern Eurasia. *Quaternary Science Reviews*, 23: 1391-1434. doi: 10.1016/j.quascirev.2003.12.007

FÜRST, J. J., NAVARRO, F., GILLET-CHAULET, F., HUSS, M., MOHOLDT, G., FETTWEIS, X., LANG, C., SEEHAUS, T., AI, S., BENHAM, T. J., BENN, D. I., BJÖRNSSON, H., DOWDESWELL, J. A., GRABIEC, M., KOHLER, J., LAVRENTIEV, I., LINDBÄCK, K., MELVOLD, K., PETTERSSON, R., RIPPIN, D., SAINTENOY, A., SÁNCHÉZ-GÁMEZ, P., SCHULER, T. V., SEVESTRE, H., VASILENKO, E. and BRAUN, M. H. (2018): The ice-free topography of Svalbard. *Geophysical Research Letters*, 45(21): 11760-11769. doi: 10.1029/2018GL079734

HEATON, T. J., KÖHLER, P., BUTZIN, M., BARD, E., REIMER, R.W., AUSTIN, W.E.N., BRONK RAMSEY, C., GROOTES, P. M., HUGHEN, K. A., KROMER, B., REIMER, P. J., ADKINS, J., BURKE, A., COOK, M. S., OLSEN, J. and SKINNER, L. C. (2020): Marine20 – The marine radiocarbon age calibration curve (0-55,000 cal BP). *Radiocarbon*, 62: 779-820. doi: 10.1017/RDC.2020.68

ISAKSEN, K., LUTZ, J., MACDONALD SØRENSEN, A., GODØY, Ø., FERRIGHI, L, EASTWOOD, S. and AABOE, S. (2022): Advances in operational permafrost monitoring on Svalbard and in Norway. *Environmental Research Letters*, 17: 095012. doi: 10.1088/1748-9326/ac8e1c

JANG, K., BAYON, G., VOGT, C., FORWICK, M., AHN, Y., KIM, J-H. and NAM, S-I. (2023): Non-linear response of glacier melting to Holocene warming in Svalbard recorded 647 by sedimentary iron (oxyhydr)oxides. *Earth and Planetary Science Letters,* 607: 118054. doi: 10.1016/j.epsl.2023. 118054

KAVAN, J. (2020a): Early twentieth century evolution of Ferdinand glacier, Svalbard, based on historic photographs and structure-from-motion technique. *Geografiska Annaler: Series A, Physical Geography*, 102(1): 57-67. doi: 10.1080/04353676.2020.1715124

KAVAN, J. (2020b): Post-little ice age development of coast in the locality of Kapp Napier, Central Spitsbergen, Svalbard archipelago. *Marine Geodesy*, 43: 234-247. doi: 10.1080/01490419.2019.1674429

KAVAN, J., TALLENTIRE, G. D., DEMIDIONOV, M., DUDEK, J. and STRZELECKI, M. C. (2022): Fifty years of tidewater glacier surface elevation and retreat dynamics along the South-East Coast of Spitsbergen (Svalbard archipelago). *Remote Sensing*, 14(2): 354. doi: 10.3390/rs14020354

KAVAN, J., STRZELECKI, M. C. (2023): Glacier decay boosts the formation of new Arctic coastal environments – Perspectives from Svalbard. *Land Degradation & Development*, 34: 3467-3474. doi: 10.1002/ldr.4695

KAVAN, J., LULÁKOVÁ, P., MAŁECKI, J. and STRZELECKI, M. C. (2024): Capturing the switch from marine to land-terminating glacier in Svalbard: 126 years of Nordenskiöldbreen retreat history. *Journal of Glaciology*, 70: 1-11. doi: 10.1017/jog.2023.92

KAVAN, J., SZCZYPIŃSKA, M., KOCHTITZKY, W., FARQUHARSON, L., BENDIXEN, M. and STRZELECKI, M. C. (2025): New coasts emerging from the retreat of Northern Hemisphere marine-terminating glaciers in the 21st century. *Nature Climate Change*, 15: 528-537. doi: 10.1038/s41558-025-02282-5

KAVAN, J., HANÁČEK, M. (2025, *this issue*): Svalbard environmental changes since the termination of the Little Ice Age: Towards warmer and less ice future. *Czech Polar Reports*.

KOEHL, J-B., ALLAART, L. (2021): The Billefjorden fault zone north of Spitsbergen: A major terrane boundary? *Polar Research*, 40: 7668. doi: 10.33265/polar.v40.7668

LONG, A. J., STRZELECKI, M. C., LLOYD, J. M. and BRYANT, C. L. (2012): Dating High Arctic Holocene relative sea level changes using juvenile articulated marine shells in raised beaches. *Quaternary Science Reviews*, 48: 61-66. doi: 10.1016/j.quascirev.2012.06.009

LULÁKOVÁ, P., ŠANTRŮČKOVÁ, H., ELSTER, J., HANÁČEK, M., KOTAS, P., MEADOR, T., TEJNECKÝ, V. and BÁRTA, J. (2023): Mineral substrate quality determines the intial soil microbial development in from of the Nordenskiöldbreen, Svalbard. *FEMS Microbiology Ecology*, 99(10): 1-15. doi: 10.1093/femsec/fiad104

MAŁECKI, J., FAUCHERRE, S. and STRZELECKI, M. C. (2013): Post−surge geometry and thermal structure of Hørbyebreen, central Spitsbergen. *Polish Polar Research*, 34: 305-321. doi: 10.2478/popore-2013-0019

MANGERUD, J. (1972): Radiocarbon dating of marine shells, including a discussion of apparent age of Recent shells from Norway. *Boreas*, 1: 143-172. doi: 10.1111/j.1502-3885.1972.tb00147.x

MANGERUD, J., GULLIKSEN, S. (1975): Apparent radiocarbon ages of recent marine shells from Norway, Spitsbergen, and Arctic Canada. *Quaternary Research,* 5: 263-273. doi: 10.1016/0033-5894(75)90028-9

MANGERUD, J., SALVIGSEN, O. (1984): The Kapp Ekholm section, Billefjorden, Spitsbergen: A discussion. *Boreas*, 13: 155-158. doi: 10.1111/j.1502-3885.1984.tb00068.x

MANGERUD, J., SVENDSEN, J. I. (1992): The last interglacial-glacial period on Spitsbergen, Svalbard. *Quaternary Science Reviews*, 11: 633-664. doi: 10.1016/0277-3791(92)90075-J

MANGERUD, J., SVENDSEN, J. I. (2018): The Holocene thermal maximum around Svalbard, Arctic North Atlantic; molluscs show early and expectational warmth. *The Holocene*, 28(1): 1-19. doi: 10.1177/0959683617715701

MARTÍN-MORENO, R., ALLENDE ÁLVAREZ, F. and HAGEN, J. O. (2017): ‘Little Ice Age’ glacier extent and subsequent retreat in Svalbard archipelago. *The Holocene*, 27: 1379-1390. doi: 10.1177/0959683617693904

MCCERERY, R., LOVELL, H., KING, O., DAVIES, B., BOSTON, C. M., MAŁECKI, J., WOODWARD, J. and CARRIVICK, J. (*in review*): Two rapidly vanishing glaciers in Svalbard: Elsabreen and Ferdinandbreen, Petuniabukta. *Annals of Glaciology*.

MÖLLER, P. (2024): A bowhead whale vertebra embedded in marine limit beach sediment on Barentsøya, Svalbard. *Polar Research*, 43: 9724. doi: 10.33265/polar.v43.9724

NORDLI, Ø., WYSZYŃSKI, P., GJELTEN, H. M., ISAKSEN, K., ŁUPIKASZA, E., NIEDŹWIEDŹ, T. and PRZYBYLAK, R. (2020): Revisiting the extended Svalbard Airport monthly temperature series, and the compiled corresponding daily series 1898–2018. *Polar Research*, 39: 3614. doi: 10.33265/polar.v39.3614

OLSSON, I. U. (1980): Content of ^{14}C in marine mammals from Northern Europe. *Radiocarbon,* 22: 662-675. doi: 10.1017/s0033822200010031

OSIKA, A., JANIA, J. and SZAFRANIEC, J. A. (2022): Holocene ice-free strait followed by dynamic Neoglacial fluctuations: Hornsund, Svalbard. *The Holocene,* 32(7): 664-679. doi: 10.1177/09596836221088232

OTTEMÖLLER, L, KIM, W-Y., WALDHAUSER, F., TJÅLAND, N. and DALLMANN, W. (2021): The Storfjorden, Svalbard, Earthquake Sequence 2008–2020: Transtensional tectonics in an Arctic intraplate region. *Seismological Research Letters*, 92: 2838-2849. doi: 10.1785/0220210022

PORTER, C., HOWAT, I., NOH, M-J., HUSBY, E., KHUVIS, S., DANISH, E., TOMKO, K., GARDINER, J., NEGRETE, A., YADAV, B., KLASSEN, J., KELLEHER, C., CLOUTIER, M., BAKKER, J., ENOS, J., ARNOLD, G., BAUER, G. and MORIN, P. (2023): "ArcticDEM, Version 4.1", Harvard Dataverse, V1, [accessed 15 December 2024]. doi: 10.7910/DVN/3VDC4W

RACHLEWICZ, G., SZCZUCIŃSKI, W. and EWERTOWSKI, M. (2007): Post−"Little Ice Age" retreat rates of glaciers around Billefjorden in central Spitsbergen, Svalbard. *Polish Polar Research*, 28: 159-186.

RANTANEN, M., KARPECHKO, A.Y., LIPPONEN, A., NORDLING, K., HYVÄRINEN, O., RUOSTEENOJA, K., VIHMA, T. and LAAKSONEN, A. (2022): The Arctic has warmed nearly four times faster than the globe since 1979. *Communications Earth & Environment*, 3: 168. doi: 10.1038/s43247-022-00498-3

SALVIGSEN, O. (1977): Radiocarbon datings and the extension of the Weichselian ice-sheet in Svalbard. *Norsk Polarinstitutt Arbok*, 1976: 209-224.

SALVIGSEN, O. (1981): Radiocarbon dated raised beaches in Kong Karls Land, Svalbard and their consequences for the glacial history of the Barents Sea area. *Geografiska Annaler Series A*, 63: 283-291. doi: 10.2307/520841

SALVIGSEN, O., ÖSTERHOLM, H. (1982): Radiocarbon dated raised beaches and glacial history of the northern coast of Spitsbergen, Svalbard. *Polar Research*, 1982(1): 97-115. doi: 10.3402/polar.v1982i1.7000

SCHOMACKER, A., FARNSWORTH, W.R., INGÓLFSSON, Ó., ALLART, L., HÅKANSSON, L., RETELLE, M., SIGGAARD-ANDERSEN, M-L, KORSGAARD, N.J., ROUILLARD, A. and KJELLMAN, S. E. (2019): Postglacial relative sea level change and glacier activity in the early and late Holocene: Wahlenbergfjorden, Nordaustlandet, Svalbard. *Scientific Reports*, 9: 6799. doi: 10.1038/s41598-019-43342-z

SESSFORD, E. G., STRZELECKI, M. C. and HORMES, A. (2015): Reconstruction of Holocene patterns of change in a High Arctic coastal landscape, Southern Sassenfjorden, Svalbard. *Geomorphology,* 234: 98-107. doi: 10.1016/j.geomorph.2014.12.046

STACHOWSKA, Z., VAN DER BILT, W.G.M. and STRZELECKI, M.C. (2024): Coastal lake sediments from Arctic Svalbard suggest colder summers are stormier. *Nature Communications*, 15: 9688. doi: 10.1038/s41467-024-53875-1

STRZELECKI, M. C., LONG, A. J., LLOYD, J. M., MAŁECKI, J., ZAGÓRSKI, P., PAWŁOWSKI, Ł. and JASKÓLSKI, M. W. (2018): The role of rapid glacier retreat and landscape transformation in controlling the post-Little Ice Age evolution of paraglacial coasts in Central Spitsbergen (Billefjorden, Svalbard). *Land Degradation & Development,* 29: 1962-1978. doi: 10.1002/ldr.2923

STRZELECKI, M.C., SZCZUCIŃSKI, W., DOMINICZAK, A., ZAGÓRSKI, P., DUDEK, J. and KNIGHT, J. (2020): New fjords, new coasts, new landscapes: The geomorphology of paraglacial coasts formed after recent glacier retreat in Brepollen (Hornsund, southern Svalbard). *Earth Surface Processes and Landforms*, 45: 1325-1334. doi: 10.1002/esp.4819

STUIVER, M., POLACH, H. A. (1977): Discussion reporting of ^{14}C data. *Radiocarbon*, 19: 355-363. doi: 10.1017/S0033822200003672

SZCZUCIŃSKI, W., ZAJACZKOWSKI, M. and SCHOLTEN, J. (2009): Sediment accumulation rates in subpolar fjords – impact of post-little ice age glaciers retreat, Billefjorden, Svalbard. *Estuarine, Coastal and Shelf Science*, 85(3): 345-356. doi: 10.1016/j.ecss.2009.08.021

TEJNECKÝ, V., LULÁKOVÁ, P., ŠANTRŮČKOVÁ, H., KŘÍŽOVÁ, P., LEHEJČEK, J., HÁJEK, T., MERCL, F., BÁRTA, J., NĚMEČEK, K. and DRÁBEK, O. (2025): Arctic willow (*Salix polaris*) exudation as a driver of microbial activity and soil formation in the high Arctic tundra. *Biogeochemistry*, 168: 30. doi: 10.1007/s10533-025-01222-x

TOMCZYK, A. M. (2021): Morphometry and morphology of fan-shaped landforms in the high-Arctic settings of central Spitsbergen, Svalbard. *Geomorphology*, 392: 107899. doi: 10.1016/j.geomorph.2021.107899

VAN DER BILT, W. G. M., D'ANDREA, W. J., WERNER, J. P. and BAKKE, J. (2019): Early Holocene temperature oscillations exceed amplitude of observed and projected warming in Svalbard lakes. *Geophysical Research Letters*, 46: 14732-14741. doi: 10.1029/2019GL084384

VAN PELT, W., FRANK, T. (2025): New glacier thickness and bed topography maps for Svalbard. *The Cryosphere*, 19: 1-17. doi: 10.5194/tc-19-1-2025

WEIDICK, A. (1972): Holocene shore-lines and glacial stages in Greenland – an attempt at correlation. *Rapport Grønlands Geologiske Undersøgelse*, 41: 1-39. doi: 10.34194/rapggu.v41.7281

YOSHIKAWA, K., NAKAMURA, T. (1996): Pingo growth ages in the delta area, Adventdalen, Spitsbergen. *Polar Record*, 32: 347-352. doi: 10.1017/S0032247400067565